Journal of Ceramic Processing Research. Vol. 27, No. 1, pp. 176~184 (2026)
(Received 8 September 2025, Received in revised form 30 October 2025, Accepted 23 December 2025)
https://doi.org/10.36410/jcpr.2026.27.1.176

J O U R N A L O F
Ceramic Processing Research

Thermal properties and nano structural analysis of potassium/lanthanum co-doped mesoporous bioactive glass

İsmail Seçkin Çardaklı*
Metallurgical and Materials Engineering, Atatürk University, Erzurum, Turkey, 25240

This study investigates the effects of potassium (K) and lanthanum (La) co-doping on mesoporous bioactive glass (BG), revealing significant modifications in its structural, thermal, and textural properties. X-ray diffraction patterns demonstrate enhanced crystallinity in K/La-BG, with prominent peaks at 33.6° and 34.2° corresponding to the (024) and (220) crystal planes, respectively. Scanning electron microscopy reveals a transition from a porous network structure in BG to densely packed, irregularly shaped particle aggregates in K/La-BG. Fourier transform infrared spectroscopy highlights changes in the Si-O-Si network (1400 cm^{-1}), Si-O bonding (800-1100 cm^{-1}), and P-O domain (600-800 cm^{-1}) regions upon doping. Thermogravimetric analysis shows improved thermal stability in K/La-BG, with a total weight loss of approximately 80% across the temperature range of 30-714 °C. Brunauer-Emmett-Teller analysis reveals a reduction in surface area from 11.54 m^2/g in BG to 8.23 m^2/g in K/La-BG, along with decreased pore volume (from 0.025 cc/g to 0.021 cc/g) and pore diameter (from 31.35 Å to 25.15 Å). These findings collectively demonstrate that K and La co-doping significantly alters the physicochemical properties of BG, potentially influencing its dissolution kinetics, bone-bonding capabilities, and overall bioactive performance in bone tissue engineering applications.

Keywords: Bioactive glass, Potassium-lanthanum co-doping, Mesoporous structure, Thermal stability, Nano structural analysis.

Introduction

Bioactive glasses (BGs) have emerged as a promising class of biomaterials for bone tissue engineering and regenerative medicine applications since their discovery by Larry Hench in the 1960s [1]. These materials, typically composed of silica, calcium oxide, sodium oxide, and phosphorus pentoxide, have garnered significant attention due to their unique ability to form strong chemical bonds with both hard and soft tissues, as well as their osteogenic and angiogenic properties [2]. In recent years, there has been a growing interest in modifying the composition of traditional BGs to enhance their performance and expand their potential applications. One such approach involves the incorporation of various dopants into the glass network. For example, the addition of potassium (K) has been shown to play a crucial role in bone metabolism and improve the biological performance of BGs [3, 4] Similarly, lanthanum (La) doping has been investigated for its ability to improve the physiochemical characteristics of the BGs, including its structural, textural, and thermal properties [5]. These enhancements suggest potential benefits for biomedical applications of BGs

The development of mesoporous BGs has been a significant advancement in the field, offering increased surface area and improved drug delivery capabilities compared to conventional BGs [6]. Several studies have explored the effects of doping MBGs with various elements to enhance their properties. Recent studies have explored the incorporation of cerium into 45S5 BG. Cerium-doped BGs have demonstrated improved redox potential and enhanced cellular bioactivity, showing potential for hard tissue therapeutic applications [7]. A novel BG composition, S53P4_MSK, incorporating magnesium, strontium and potassium, has shown high sinterability without crystallization at 700 °C, along with good mechanical properties and bioactivity [8]. Boron-containing BGs have shown potential for muscle regeneration. In vitro studies indicated that muscle-related gene expressions increased more for boron-doped glasses compared to traditional 45S5 BG [9]. Copper (Cu) and Zinc (Zn) doped BGs have been investigated for their antibacterial and angiogenic properties. These dopants have been shown to modify the degradation profile and mechanical properties of polymer/glass composite scaffolds [10]. The incorporation of multiple therapeutic ions and the development of composite materials combining BGs with polymers or other ceramics are areas of active investigation [8].

Recent studies demonstrate that compositional tuning with alkali, rare-earth, and transition-metal ions effectively tailors the structure and biological performance of bioactive glasses (BGs). Substitution of Na^+ or Ca^{2+}

*Corresponding author:
Tel : +90 505 929 14 17
Fax: +90 442 231 4910
E-mail: cardakli@atauni.edu.tr

with K^+, Mg^{2+}, or La^{3+} modifies network connectivity, enhances densification, and improves thermal stability and bioactivity [11-13]. Potassium- and La-doped BGs show increased surface reactivity, hydroxyapatite formation, and osteogenic potential, while optimized B_2O_3/Al_2O_3 ratios enhance dissolution control and cytocompatibility [11-13].

Furthermore, transition-metal doping strengthens the mechanical and biological functionality of BGs. Zn and Co ions regulate dissolution and stimulate osteogenic and angiogenic responses, whereas Mn promotes collagen formation and mineralization [12, 14, 15]. Na_2O, Fe^{3+}, and Mg^{2+} additions also increase ion exchange and thermal stability through network cross-linking [16]. Overall, controlled multi-element doping provides a versatile route to tune network polymerization, ionic mobility, and degradation kinetics—achieving improved bioactivity and osteoconductivity in next-generation bioactive glass systems.

Previous studies have reported that compositional modification of bioactive glass systems significantly affects apatite formation and cellular response [13]. Noris-Suárez et al. demonstrated that oxide-modified silicate glasses promote SiO_2-rich layer formation followed by Ca–P deposition and osteoblastic mineralization behavior [13]. In addition, bioglass-reinforced hydroxyapatite composites were shown to enhance mechanical stability while maintaining bioactivity [17]. These findings highlight the importance of controlled compositional design in bioactive ceramic systems.

Despite these advancements, significant challenges remain in optimizing the composition and structure of BGs for specific biomedical applications. The complex interplay between glass composition, nanostructure, and biological performance necessitates a multidisciplinary approach, combining materials science, biology, and medicine. Moreover, the translation of these advanced materials from the laboratory to clinical practice requires rigorous evaluation of their long-term safety and efficacy. As we stand on the cusp of a new era in biomaterials science, the potential of BGs to address unmet clinical needs has never been greater. This study aims to contribute to this rapidly evolving field by investigating the thermal properties and nano structural characteristics of K and La ions co-doped mesoporous BGs. By elucidating the fundamental relationships between composition, structure, and properties, we hope to pave the way for the development of next-generation biomaterials with enhanced performance and expanded therapeutic applications.

Materials and Methods

The synthesis of BG and K/La co-doped BG employed a sol-gel methodology, utilizing an array of precursor compounds to yield the desired oxide components. The silicon source, tetraethyl orthosilicate (TEOS, $SiC_8H_{20}O_4$, Merck), underwent hydrolysis in an acidic aqueous medium, initiating the sol-gel process. Concurrently, triethyl phosphate (TEP, $C_6H_{15}O_4P$, Merck), calcium nitrate tetrahydrate ($Ca(NO_3)_2{\cdot}4H_2O$, Merck), sodium nitrate ($NaNO_3$, Merck), potassium nitrate (KNO_3, Merck) and lanthanum nitrate hexahydrate ($La(NO_3)_3{\cdot}6H_2O$, Merck) were incorporated to introduce phosphorus, sodium, calcium, potassium and lanthanum elements, respectively.

The synthesis process began with the preparation of a dilute nitric acid solution, which was subsequently combined with a larger volume of water. The initiation of TEOS (33.5mL) hydrolysis occurred upon its addition to this acidic aqueous mixture. This reaction was allowed to proceed for an hour to ensure thorough hydrolysis. Concurrently, a separate set of precursor materials was prepared and homogenized over a 45-minute period. These additional components included precise quantities utilized were 2.9 mL of TEP, 13.52 g of sodium nitrate, and 20.13 g of calcium nitrate.

The synthesis process involved the meticulous preparation and combination of distinct precursor materials to yield a transparent colloidal suspension. This sol was subsequently transferred to a vessel and allowed to remain undisturbed at ambient temperature for a period of 5 days, facilitating the crucial gelation phase. This step is pivotal as it initiates the formation of a characteristic three-dimensional network structure within the gel. Following the gelation process, the resultant gel underwent a 24-hour maturation period at 70 °C in a sealed environment. This aging step serves to reinforce and consolidate the gel's internal network structure. Subsequently, the matured gel was subjected to a desiccation process, involving exposure to 120 °C for a duration of 24 hours in a controlled heating apparatus to eliminate residual moisture. The final stage of the synthesis protocol involved a thermal treatment designed to eradicate any lingering nitrate compounds. Complete removal of nitrate residues was confirmed by FTIR spectroscopy and thermogravimetric analysis. The absence of the characteristic NO_3^- stretching band at approximately 1384 cm^{-1} in FTIR spectra and the stabilization of the TGA curve beyond 700 °C together verified that nitrate species were entirely decomposed after calcination.

The incorporation of K and La into the BG particles was achieved using the same methodological approach and parameters. However, this process included additional steps. After the addition of calcium nitrate, 0.02 mole of potassium nitrate was introduced to the mixture for K-doped BG. For K/La-doped BG, 0.02 mole of lanthanum nitrate was added following the calcium nitrate incorporation. These modifications to the standard BG synthesis procedure allowed for the successful doping of the BG particles with K and La ions, respectively, while maintaining the overall synthesis parameters and thermal treatment process. The dopant concentrations

(0.02 mol KNO_3 and 0.02 mol $La(NO_3)_3 \cdot 6H_2O$) were selected based on preliminary trials and previous reports indicating that lower dopant levels (< 0.05 mol) maintain glass homogeneity while enabling noticeable structural modification [18].

The BG samples, including those doped with K/La-BG, underwent comprehensive characterization using an array of sophisticated analytical techniques. X-ray diffraction analysis, performed on a Rigaku Ultima IV diffractometer, provided insights into the materials' phase composition and crystallinity. The XRD measurements employed a meticulous scanning protocol, covering a 2θ range of 20° to 80° with precise 0.03° increments. To elucidate the chemical structure and functional groups present in the powders, Fourier transform infrared spectroscopy was conducted using a Bruker IFS66/S spectrometer. This method yielded unique spectral signatures for each molecular component, offering valuable information about the samples' chemical composition. Morphological examination and elemental analysis were carried out using a Quanta 400F field emission scanning electron microscope equipped with elemental mapping capabilities. To prepare the samples for FESEM imaging, the powders underwent a dispersion process. This involved dissolving the materials in ethanol, followed by a 30-minute sonication treatment to disrupt particle aggregates. The resulting suspension was then allowed to dry at ambient temperature before imaging.

The thermal behavior and compositional changes of the materials were evaluated using thermogravimetric analysis (TGA) on a PerkinElmer Pyris 1 instrument. This technique monitored mass fluctuations as the samples were heated from ambient temperature to 950 °C, providing insights into their thermal stability and decomposition patterns. To characterize the textural properties of the powdered samples, a multipoint Brunauer-Emmett-Teller (BET) analysis was conducted using a Quanta chrome Corporation Autosorb 6 apparatus. This method yielded crucial information about the samples' specific surface area, pore size distribution, and total pore volume. These parameters are fundamental in determining the adsorption characteristics of the powders, which play a vital role in their potential applications across various industries

Results and Discussion

The XRD patterns reveal significant structural characteristics of both the BG and K/La-BG (Fig. 1). The diffraction patterns primarily correspond to two major crystalline phases: $Na_2Ca_2Si_3O_9$ (combeite, JCPDS #075-1687) and $Na_2Ca_4(PO_4)_2SiO_4$ (JCPDS #032-1053) [4]. The most prominent peaks appear at 33.6° and 34.2°, corresponding to the (024) and (220) crystal planes respectively, indicating well-developed crystalline structures.

The incorporation of K and La ions into the BG structure leads to several notable modifications. The addition of dopants results in increased peak intensities, providing strong evidence of successful incorporation into the glass network. This enhancement in peak intensity suggests improved crystallinity of the overall structure [4, 5]. A distinct peak shift toward lower two-theta values indicates lattice expansion. This shift can be attributed to the ionic replacement of Ca^{2+} ions (radius 0.100 nm) with larger K^+ ions (radius 0.133 nm). The introduction of La^{3+} ions enhances the crystallinity of diffraction peaks and modifies the glass network structure. The combined effect of K and La doping leads to Formation of new crystalline phases, and modified glass network connectivity.

The detected crystalline phases—$Na_2Ca_2Si_3O_9$ (combeite)

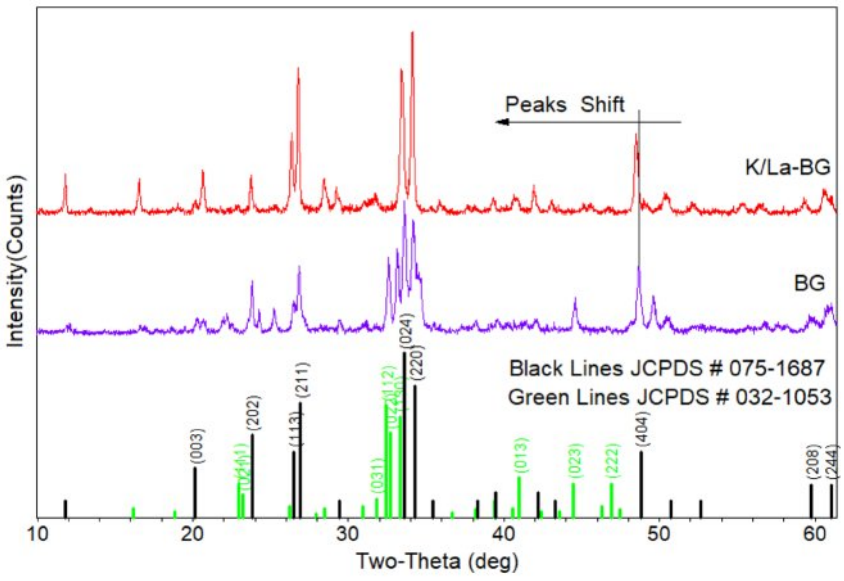

Fig. 1. XRD pattern of BG and K/La-BG particles.

and $Na_2Ca_4(PO_4)_2SiO_4$—are bioactive components known to promote controlled Ca^{2+} and Si^{4+} ion release, facilitating hydroxyapatite formation on the glass surface. Their presence suggests improved mechanical stability and enhanced interfacial bonding potential with bone tissue, thereby supporting the biofunctional significance of K/La co-doping.

The SEM micrographs demonstrate striking morphological distinctions between the conventional BG and K/La-BG samples (Fig. 2). The traditional BG exhibits a distinctive three-dimensional network characterized by uniformly distributed interconnected pores and a notably rough surface texture. This architectural arrangement, typical of sol-gel synthesized BGs, creates an amorphous structure where the interconnected porosity plays a crucial role in enhancing the material's bioactive properties [19-21]. In contrast, the K/La-BG composition reveals a markedly altered microstructure. The incorporation of K and La ions leads to the formation of densely packed, irregularly shaped particle aggregates. These particles demonstrate a pronounced tendency toward clustering, resulting in a more compact structure with noticeably reduced porosity compared to the undoped BG [2, 22]. The crystallite dimensions appear significantly smaller, organizing themselves into distinctive cluster-like formations throughout the material's surface. The structural modifications induced by K and La doping extend beyond mere morphological changes. The transformation from spherical to aggregated particle morphology can be attributed to the network-modifying effects of La ions incorporation. This doping process not only enhances the material's crystallinity but also fundamentally alters the microstructural organization of the bioglass matrix [23]. Quantitative particle-size estimation using ImageJ software on multiple SEM micrographs yielded an average size of 210 ± 40 nm for the undoped BG and 190 ± 35 nm for the K/La-BG particles. The reduction in average particle size corresponds to the enhanced nucleation tendency induced by dopant incorporation, which contributes to the observed densification of aggregates.

The synergistic effect of K and La ions results in a more consolidated structure, departing significantly from the traditional BG architecture. These substantial morphological alterations suggest profound changes in the material's physicochemical properties, potentially influencing its dissolution kinetics and bone-bonding capabilities in physiological environments. The modified structural characteristics are likely to play a crucial role in determining the material's overall bioactive performance and its effectiveness in bone tissue engineering applications.

The elemental mapping analysis provides compelling evidence of distinct compositional variations between the conventional BG and K/La-BG systems (Fig. 3). A comprehensive examination reveals the uniform distribution of fundamental elements (Si, Ca, P, and Na) throughout both glass matrices, demonstrating successful synthesis of the base structure. In the K/La-BG composition, the detection of well-distributed K and La signals confirms their effective incorporation into the glass network during the sol-gel synthesis process. The uniform spatial distribution of La^{3+} ions throughout the glass matrix is particularly significant, as it indicates their role as network modifiers, fundamentally altering the glass structure at the atomic level. The consistent elemental distribution patterns align with the observed morphological characteristics, suggesting that the structural modifications induced by K and La incorporation occur uniformly throughout the material, resulting in a well-integrated glass system with modified physicochemical properties.

The FTIR spectra reveal distinct structural characteristics between the BG and K/La-BG (Fig. 4). The spectra can be divided into three main regions: (i) Si-O-Si Network (1400 cm^{-1}), (ii) Si-O Bonding Region (800-1100 cm^{-1}), and (iii) P-O Domain (600-800 cm^{-1}) [4]. In the Si-O-Si network region, the K/La-BG displays a sharper peak compared to the broader peak in BG. This modification indicates a significant change in the silicate network structure upon doping, suggesting altered network connectivity and bond arrangements. In the Si-O Bonding Region, K/La-BG exhibits a

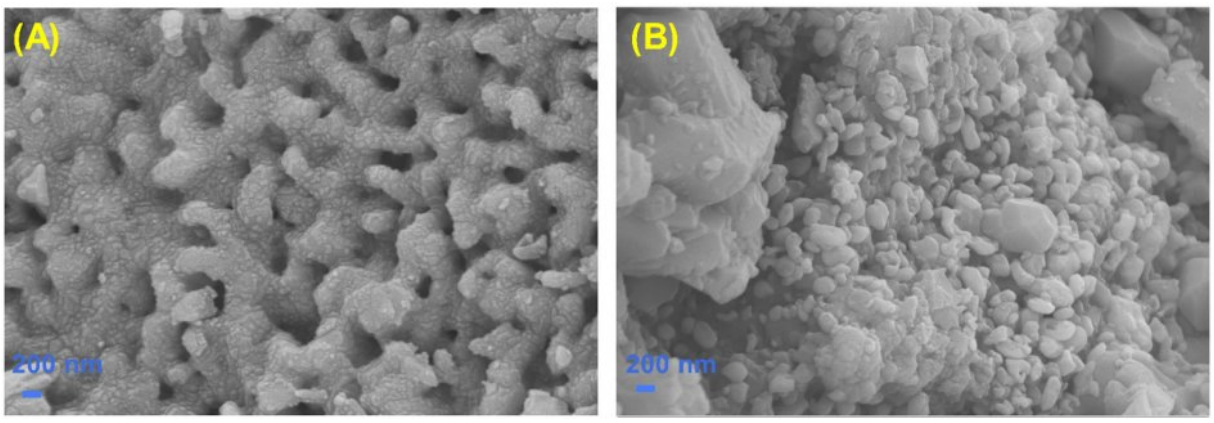

Fig. 2. SEM images of (A) BG, and (B) K/La-BG particles.

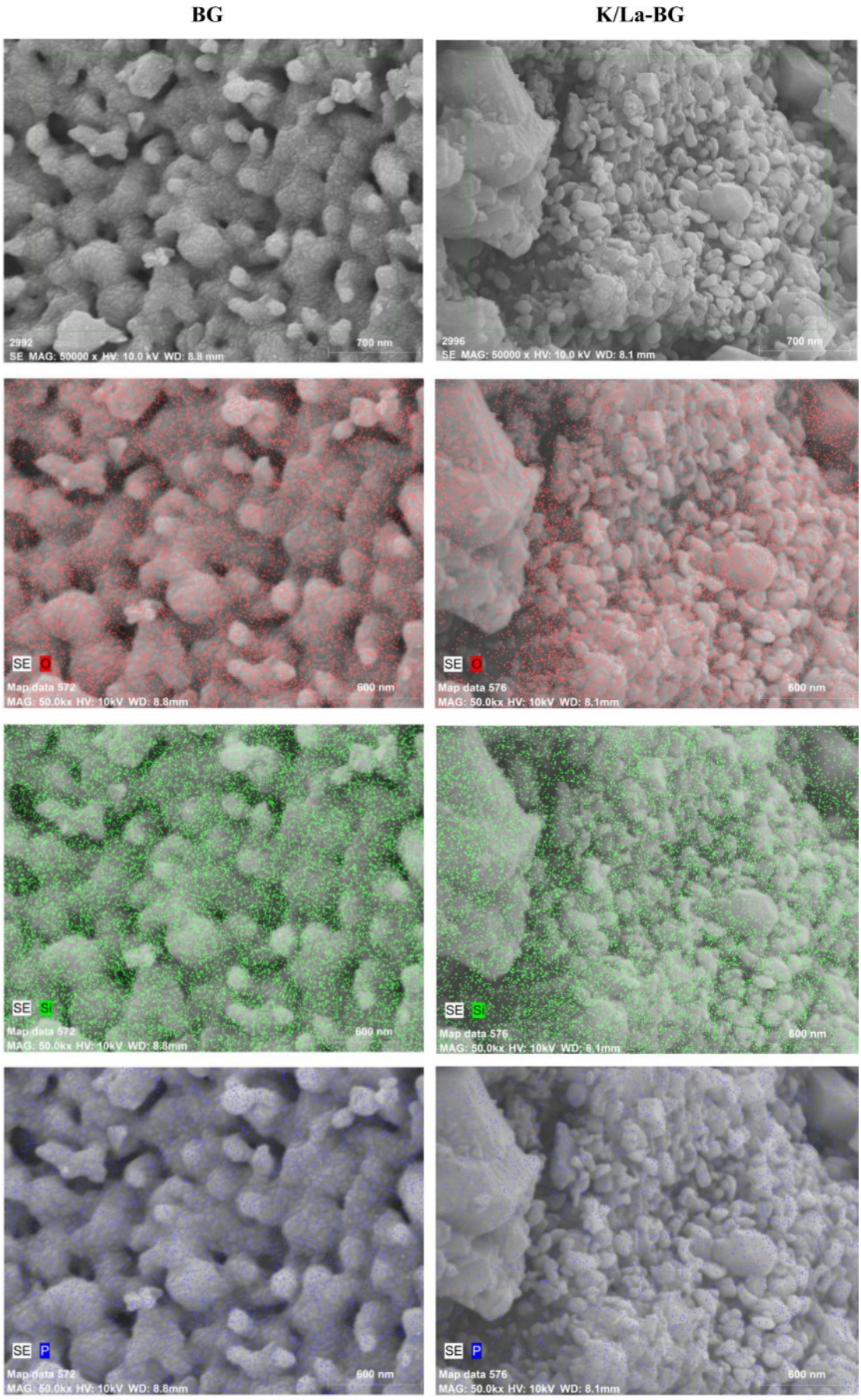

Fig. 3. FESEM images and elemental mapping of BG and K/La-BG materials.

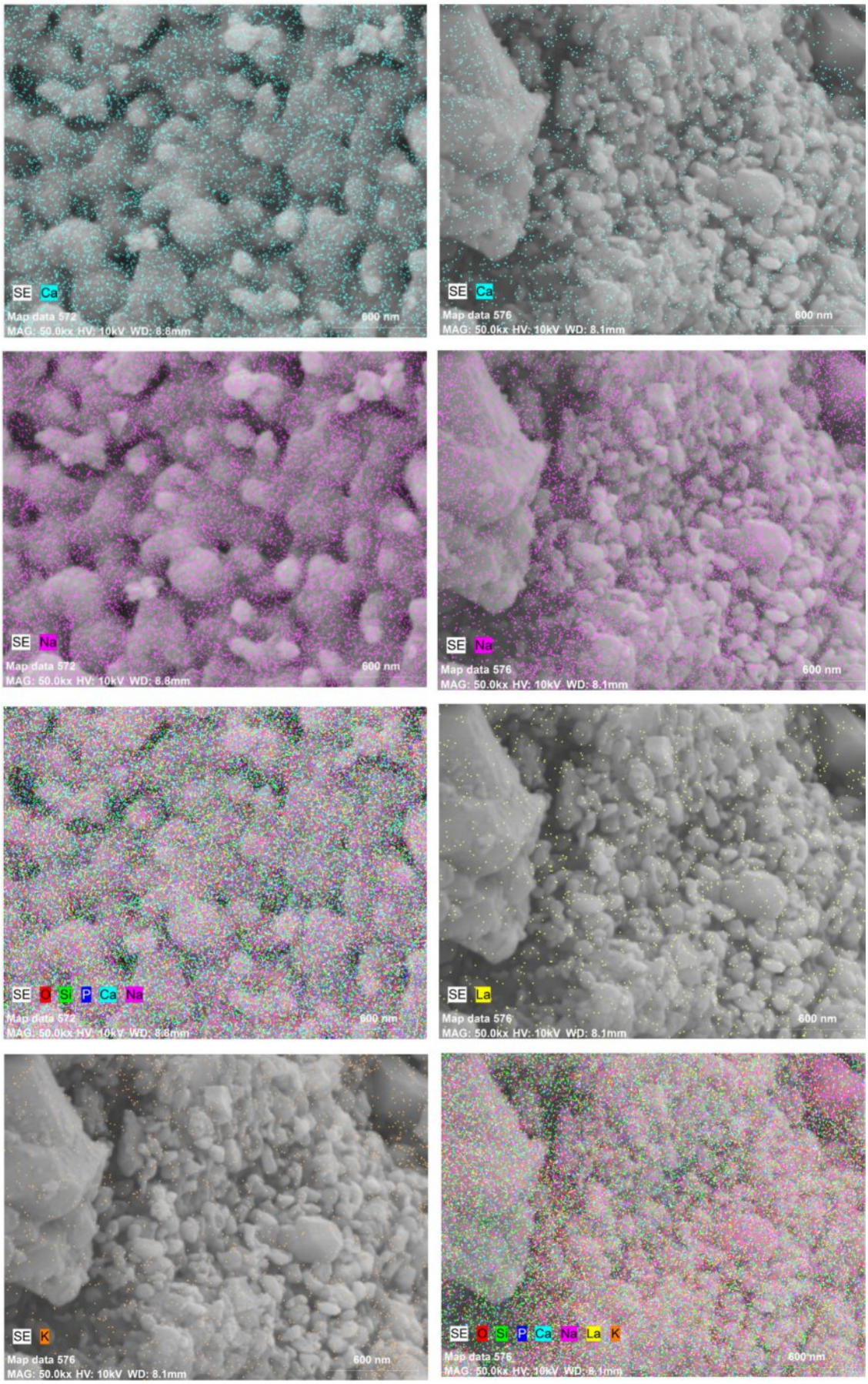

Fig. 3. Continued.

distinctive double peak pattern, contrasting with the single broader peak seen in the undoped BG. This peak splitting phenomenon demonstrates the creation of new chemical environments around silicon-oxygen bonds. The increased peak definition suggests a more ordered local structure in specific regions while maintaining the overall amorphous nature of the glass. The P-O Domain shows notable changes with K/La doping. The more pronounced peaks in K/La-BG indicate a restructured phosphate environment. This modification is particularly attributed to the influence of La^{3+} ions, which alter the local coordination environment around phosphate groups. The introduction of K^+ and La^{3+} ions create substantial changes in the glass network. While K^+ acts as a conventional network modifier, La^{3+}'s higher charge state produces more significant structural modifications. Together, these ions create a more complex glass structure with modified bond angles and connectivity patterns, which can influence the material's bioactive properties [24].

The TGA curves for both BG and K/La-BG materials show three distinct temperature regions with different weight loss characteristics (Fig. 5). Region A (30-151 °C) is associated with desorption of physically adsorbed water molecules from the surface, with both materials showing similar initial weight loss patterns [18]. Region B (151-264 °C) corresponds to the loss of lattice water and decomposition of organic constituents, where K/La-BG shows slightly higher stability compared to undoped BG. Region C (264-714 °C) is characterized by the breakdown and release of nitrate entities from the glass matrix, with K/La-BG demonstrating improved thermal stability and reduced weight loss [18]. The total weight loss for both materials is approximately 80% across the temperature range, with K/La-BG showing better thermal stability and less weight loss compared to undoped BG. The addition of K and La ions appears to enhance the thermal stability of the glass structure. Lanthanum oxide incorporation has been shown to enhance glass transition temperature and thermal stability, while K doping affects the thermal degradation profile by reducing weight loss across all temperature ranges. The improved thermal stability suggests a more crystalline structure in the K/La-BG composite. The enhanced thermal stability of K/La-BG materials has important implications, including better structural integrity during processing and application, improved potential for biomedical applications requiring thermal resistance, and enhanced chemical stability in biological environments [8, 12]. This analysis aligns with previous studies showing that ion doping can significantly improve the thermal properties of BGs while maintaining their bioactive characteristics.

The BET analysis reveals significant structural differences between pure BG and K/La-doped BG as evidenced by both the isotherm curves and surface characterization data (Fig. 6). The N_2 adsorption-desorption isotherms display Type IV behavior with H1 hysteresis loops, characteristic of mesoporous materials [20, 25]. The pure BG demonstrates superior N_2 adsorption capacity throughout the pressure range, reaching a maximum adsorbed volume of approximately 14 cc/g at high relative pressures (P/P_0 approaching 1.0). This correlates with its higher surface area of 11.54 m^2/g compared to 8.23 m^2/g for K/La-BG (Table 1). The pore structure analysis through BJH method shows that K/La

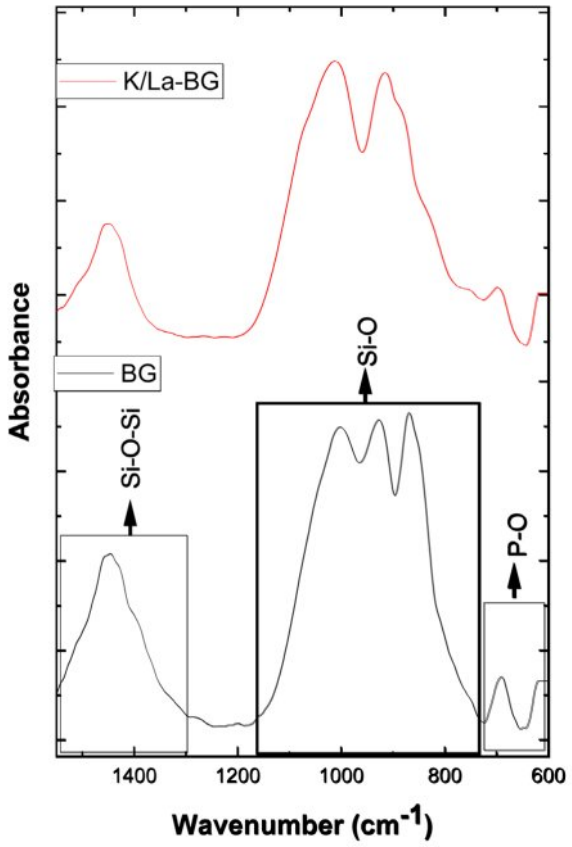

Fig. 4. FTIR spectra of BG and K/La-BG materials.

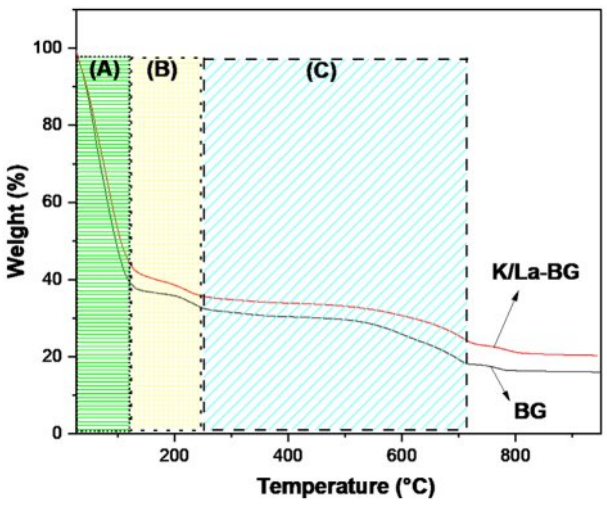

Fig. 5. TGA graph of the BG and K/La-BG materials.

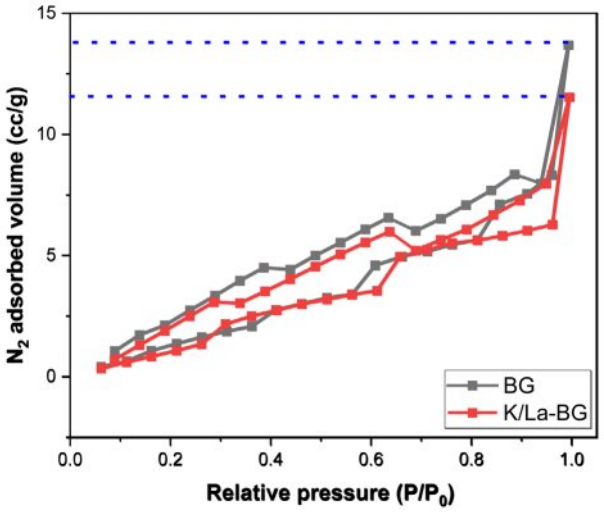

Fig. 6. N_2 adsorption–desorption isotherm.

doping induces a notable modification in the material's porosity. The cumulative adsorption pore volume decreases from 0.025 cc/g in pure BG to 0.021 cc/g in K/La-BG, while the desorption pore volume similarly reduces from 0.029 cc/g to 0.025 cc/g. This reduction in pore volume is accompanied by a significant decrease in the adsorption pore diameter from 31.35 Å to 25.15 Å, though interestingly, the desorption pore diameter remains almost unchanged at approximately 21.33 Å. The isotherm curves further illustrate the impact of K/La doping, showing a reduced hysteresis loop area and a more gradual increase in adsorbed volume with pressure for the doped sample. This suggests that the incorporation of K and La ions modifies the glass network structure, leading to a more condensed material with reduced porosity. The smaller hysteresis loop in K/La-BG indicates a more uniform pore size distribution, despite the overall reduction in pore volume and surface area. These structural modifications likely influence the material's mechanical properties and ion exchange capabilities, which are crucial for its potential biomedical applications.

These observations are consistent with several recent studies on doped BGs. A study on boron-doped mesoporous BG nanoparticles found that doping altered the pore structure, with changes in pore size distribution and surface area depending on the doping concentration [9]. Research on Mg-doped mesoporous BG nanoparticles showed that increasing Mg content led to changes in specific surface area and pore volume, indicating modifications to the glass network structure [18]. An investigation of Zn and Ag co-doped BG nanoparticles revealed that doping can affect the glass network connectivity, potentially leading to changes in particle morphology and porosity [26]. Furthermore, a comprehensive review of ion substitution in BG highlighted that the incorporation of various ions can significantly alter the glass network structure, affecting properties such as porosity and surface area [27]. Research on strontium and lithium doped BG scaffolds demonstrated that doping can modify the physico-chemical properties of the glass, including its microstructure and porosity [28]. These studies collectively support the observation that doping BGs with ions like K and La can lead to significant changes in the glass network structure, resulting in alterations to porosity, pore size distribution, and surface area.

Conclusion

This study investigates the effects of potassium (K) and lanthanum (La) co-doping on mesoporous bioactive glass (BG), revealing significant modifications in its structural, thermal, and textural properties compared to conventional BG. XRD patterns demonstrate enhanced crystallinity and the formation of new crystalline phases in K/La-BG, indicating successful incorporation of dopants into the glass network. SEM micrographs show a transition from a porous network structure in BG to densely packed, irregularly shaped particle aggregates in K/La-BG, suggesting altered bioactive properties. Elemental mapping confirms the uniform distribution of K and La throughout the glass matrix. FTIR spectroscopy highlights significant changes in the silicate network structure and phosphate environment upon doping, indicating modified bond arrangements and local coordination. Thermogravimetric analysis demonstrates improved thermal stability in K/La-BG, particularly in the higher temperature ranges. BET analysis reveals a reduction in surface area, pore volume, and pore diameter in K/La-BG, suggesting a more

Table 1. Textural parameters obtained by the N_2 adsorption measurement.

ID	Surface Area	Pore Volume Data		Pore Size Data	
		BJH Method CAPV*	BJH Method CDPV#	BJH Method APD**	BJH Method DPD#*
BG	11.54 m^2/g	0.025 cc/g	0.029 cc/g	31.35 Å	21.33 Å
K/La-BG	8.23 m^2/g	0.021 cc/g	0.025 cc/g	25.15Å	21.32 Å

*Cumulative Adsorption Pore Volume: CAPV
#Cumulative Desorption Pore Volume: CDPV
**Adsorption Pore Diameter: APD
#*Desorption Pore Diameter: DPD

condensed material structure.

In summary, K and La co-doping markedly modified the structural, thermal, and textural features of the mesoporous bioactive glass. The enhanced crystallinity and reduced porosity imply a denser and more stable network, which may improve mechanical robustness and regulate dissolution behavior. The synergy between K^+ and La^{3+} ions is expected to yield superior bioactive and osteogenic performance. Future work will include in-vitro bioactivity and ion-release studies in simulated body fluid to further evaluate the biomedical potential of K/La-BG composites.

References

1. M.N. Rahaman, D.E. Day, B.S. Bal, Q. Fu, S.B. Jung, L.F. Bonewald, and A.P. Tomsia, Acta Biomater. 7[6] (2011) 2355-2373.
2. M.H. Kaou, M. Furkó, K. Balázsi, and C. Balázsi, Nanomaterials 13[16] (2023) 2287.
3. D. Bellucci, V. Cannillo, and A. Sola, Ceram. Int. 37[1] (2011) 145-157.
4. A.Z. Alshemary, A.B. Naser, S.M. Haidary, and İ.S. Çardaklı, Ceram.–Silikáty 68[3] (2024) 353-359.
5. A.Z. Ashemary, S.M. Haidary, Y. Muhammed, and İ.S. Çardaklı, Dig. J. Nanomater. Biostructures 18[2] (2023) 681-688.
6. M. Vallet-Regí, M. Colilla, I. Izquierdo-Barba, C. Vitale-Brovarone, and S. Fiorilli, Pharmaceutics 14[12] (2022) 2636.
7. J.-H. Ryu, T.-Y. Kang, S.-H. Choi, J.-S. Kwon, and M.-H. Hong, Sci. Rep. 14[1] (2024) 15837.
8. A. Martelli, D. Bellucci, and V. Cannillo, Materials 17[24] (2024) 6175.
9. D. Ege, Q. Nawaz, A.M. Beltrán, and A.R. Boccaccini, ACS Biomater. Sci. Eng. 8[12] (2022) 5273-5283.
10. J. Bejarano, R. Detsch, A.R. Boccaccini, and H. Palza, J. Biomed. Mater. Res. A 105[3] (2017) 746-756.
11. M. Shoaib, A. Saeed, J. Akhtar, M.S.U. Rahman, A. Ullah, K. Jurkschat, and M.M. Naseer, Mater. Sci. Eng. C 75 (2017) 836-844.
12. F.G. Mecca, D. Bellucci, and V. Cannillo, Materials 16[13] (2023) 4651-4663.
13. K. Noris-Suárez, M. Vasquez, Y. López, T. San Antonio, I. Barrios de Arenas, and J. Lira-Olivares, J. Ceram. Process. Res. 11[2] (2010) 129-137.
14. F. Baino, E. Fiume, S. Barberi, and C. Vitale-Brovarone, Materials 16[14] (2023) 4994.
15. M. Curcio, F. Branda, M. Malucelli, and S. D'Urso, Coatings 12[10] (2022) 1427.
16. T. Charoensuk, C. Sirisathitkul, U. Boonyang, I.J. Macha, Y. Sirisathitkul, and B. Ben-Nissan, J. Ceram. Process. Res. 17[7] (2016) 742-746.
17. N. Ekren, J. Ceram. Process. Res. 18[1] (2017) 64-68.
18. Z. Tabia, K.E. Mabrouk, M. Brichaa, and K. Nounehb, RSC Adv. 9[22] (2019) 12232-12246.
19. L.M. Mukundan, R. Nirmal, D. Vaikkath, and P.D. Nair, Biomatter 3[2] (2013) e24288.
20. K. Aneb, H. Oudadesse, H. Khireddine, B. Lefeuvre, O. Merdrignac-Conanec, F. Tessier, and A. Lucas, Mater. Today Commun. 34 (2023) 104992.
21. T.H. Dang, T.H. Bui, E.V. Guseva, A.T. Ta, A.T. Nguyen, T.T.H. Hoang, and X.V. Bui, Crystals 10[6] (2020) 529.
22. H.E. Skallevold, D. Rokaya, Z. Khursid, and M.S. Zafar, Int. J. Mol. Sci. 20[23] (2019) 5960.
23. U. Pantulap, M. Arango-Ospina, and A.R. Boccaccini, J. Mater. Sci.: Mater. Med. 33[1] (2022) 3.
24. S. Kargozar, F. Kermani, S.M. Beidokhti, S. Hamzehlou, E. Verné, S. Ferraris, and F. Baino, Materials 12[22] (2019) 3696.
25. M. Schumacher, P. Habibovic, and S. Van Rijt, Bioact. Mater. 6[7] (2021) 1921-1931.
26. P. Naruphontjirakul, P. Kanchanadumkerng, and P. Ruenraroengsak, Sci. Rep. 13[1] (2023) 6775.
27. S.M. Rabiee, N. Nazparvar, M. Azizian, D. Vashaee, and L. Tayebi, Ceram. Int. 41[6] (2015) 7241-7251.
28. P.K. Khan, A. Mahato, B. Kundu, S.K. Nandi, P. Mukherjee, S. Datta, S. Sarkar, J. Mukherjee, S. Nath, V.K. Balla, and C. Mandal, Sci. Rep. 6[1] (2016) 32964.